On the observability of finite-depth short-crested water waves

By M. IOUALALEN[1]†, A. J. ROBERTS[2] AND C. KHARIF[3]

[1] Groupe SURTROPAC, Institut Français de Recherche Scientifique pour le Développement en Coopération (ORSTOM), BP A5, Nouméa, New-Caledonia

[2] Department of Mathematics and Computing, University of Southern Queensland, Toowoomba, Queensland, 4350 Australia

[3] Institut de Recherche sur les Phénomènes Hors Equilibre, LIOA, 163 avenue de Luminy, Case 903, 13288 Marseille cedex 9, France

A numerical study of the superharmonic instabilities of short-crested waves on water of finite depth is performed in order to measure their time scales. It is shown that these superharmonic instabilities can be significant – unlike the deep-water case – in parts of the parameter regime. New resonances associated with the standing wave limit are studied closely. These instabilities 'contaminate' most of the parameter space, excluding that near two-dimensional progressive waves; however, they are significant only near the standing wave limit. The main result is that very narrow bands of both short-crested waves 'close' to two-dimensional standing waves, and of well developed short-crested waves, perturbed by superharmonic instabilities, are unstable for depths shallower than approximately a non-dimensional depth $d = 1$; the study is performed down to depth $d = 0.5$ beyond which the computations do not converge sufficiently. As a corollary, the present study predicts that these very narrow sub-domains of short-crested wave fields will not be observable, although most of the short-crested wave fields will be.

1. Introduction

For over two decades, water waves and their stability have been the subject of very intensive study in terms of direct measurements, of computations and from a theoretical point of view. Many authors have contributed to a better understanding of water wave motion; most have focused their analysis on two-dimensional progressive Stokes waves. The study of pure Stokes waves is now nearly complete, except for the development of wave breaking which is a major aspect of interest. All these studies appear to be very helpful if one intends to extend analysis to more complex flows, like standing waves or three-dimensional waves, since the results obtained and the numerical and experimental procedures are clearly settled. The study of three-dimensional waves is developing because (i) it provides a more realistic description of the ocean and (ii) the field of research has been clarified, especially since Roberts (1983) described some evolution properties like harmonic resonances, which occur in a symmetrical and monophase short-crested wave field. These waves may be produced by a sea-wall reflection of a two-dimensional progressive wave field propagating at an

angle θ to the normal to the wall, or by two two-dimensional progressive waves of the same frequency and the same wavelength intersecting at an angle γ so that $\theta = (\pi - \gamma)/2$. These pure short-crested wave forms have been calculated: Fuchs (1952) obtained second-order solutions, Chappelear (1961) extended them to third order. Hsu, Tsuchiya & Silvester (1979) also calculated a third-order expansion in dimensionless form for water of finite depth. These solutions were extended analytically by Ioualalen (1993) up to the fourth (and fifth) order using an algebraic manipulator. Roberts & Peregrine (1983) calculated a sixth-order expansion for long-crested waves, while Roberts (1983) and Marchant & Roberts (1987) computed highly nonlinear short-crested waves using a perturbation method up to 27th and 35th orders respectively for deep water and finite-depth water respectively. Fully numerical computations have been performed by Roberts & Schwartz (1983) and Bryant (1985). One of the properties of these waves, absent in Stokes waves, is the occurrence of harmonic resonance. Roberts (1983) described how the perturbation series has everywhere a zero radius of convergence. However, he could extract some useful results, use Padé approximation to detect poles of truncated series, and the Shanks transform to attain numerical convergence for finite-amplitude waves. From his analysis, he deduced that most of these resonances are of very high order: the error produced by a truncation at order N of the series expansion (and so ignoring all the higher-order resonances) is of order $h^{N/3}$, where h is the wave steepness. This relatively good accuracy is not surprising since pole-zero pairs are extremely close together, showing the weakness of the resonances. This result was confirmed by Ioualalen & Kharif (1993, 1994, hereafter referred to as IK 93, 94), who showed that instabilities associated with these harmonic resonances occur as sporadic 'bubbles' of instability. The authors explained the generation of these instabilities as a collision of two superharmonic modes at zero frequency, their growth rates being very weak compared to subharmonic instabilities. The strongest superharmonic growth rates are at least two orders in h lower than the subharmonic ones. This result suggests that these resonances are unlikely to be significant because they will not have time to develop, as subharmonic instabilities have a much more rapid growth. The results on subharmonic time scales were confirmed by Badulin *et al.* (1995) using a Hamiltonian weakly nonlinear formulation.

The purpose of the present study is to extend the work reported in IK 93 to water of finite depth. The harmonic resonances do not vanish, but one can expect that their time scales will be modified since the wave dispersion depends on the water depth d. This study was also motivated by the emergence of new harmonic resonances arising for finite depth, in particular in the vicinity of the standing wave limit $\theta = 0°$ – resonances noted by Mercer & Roberts (1994) in computations of finite-depth standing waves. These new instabilities, perhaps due to the weakly dispersive nature of shallow-water waves, persist for angles where the three-dimensionality is well developed, see Marchant & Roberts (1987).

Experiments on finite-depth short-crested waves have been performed by Hammack, Scheffner & Segur (1989, 1991) and Hammack *et al.* (1995), and their occurrence noted by Peregrine (1985). Both suggest that short-crested waves are observable over a certain time when the waves do not change their shape. In the present numerical study, quantitative comparisons with these experiments are performed and investigations are carried out to determine whether the waves are typically unsteady for some ranges of depths d and angles θ.

2. Mathematical formulation

2.1. *Introduction*

We consider short-crested surface gravity waves on an inviscid incompressible fluid of finite depth, where the flow is assumed irrotational. The governing equations are

$$\nabla^2\phi = 0 \qquad\qquad \text{for} \quad -d \leqslant z \leqslant \eta(x,y,t), \qquad (2.1)$$

$$\phi_z = 0 \qquad\qquad \text{on} \quad z = -d, \qquad (2.2)$$

$$\left.\begin{array}{l} \phi_t + \eta + \tfrac{1}{2}(\phi_x^2 + \phi_y^2 + \phi_z^2) = 0 \\ \eta_t + \phi_x\,\eta_x + \phi_y\,\eta_y - \phi_z = 0 \end{array}\right\} \quad \text{on} \quad z = \eta(x,y,t), \qquad (2.3)$$

$$(2.4)$$

where d is the depth of the fluid, $\phi(x,y,z,t)$ is the velocity potential and $z = \eta(x,y,t)$ is the equation of the free surface. As in Hsu *et al.* (1979), equations (2.1)–(2.4) are given in a dimensionless form with respect to the reference length $1/k$ and the reference time $(gk)^{-1/2}$, where g is the gravitational acceleration and k the wavenumber of the incident wave train.

In order to perform the linear stability analysis, we define a reference frame where steady solutions $(\bar{\eta}, \bar{\phi})$ of equations (2.1)–(2.4) are available. Define a frame of reference (x^*, y^*, z^*, t^*), so that $x^* = x - ct$, $y^* = y$, $z^* = z$ and $t^* = t$; c is the celerity of the propagating wave train and is equal to ω/α, ω being the frequency of the wave and $\alpha = \sin\theta$ is the x-wavenumber, the y-wavenumber being $\beta = \cos\theta$. Following IK 93, define

$$\eta(x^*, y^*, t^*) = \bar{\eta}(x^*, y^*) + \eta'(x^*, y^*, t^*), \qquad (2.5)$$

$$\phi(x^*, y^*, z^*, t^*) = \bar{\phi}(x^*, y^*, z^*) + \phi'(x^*, y^*, z^*, t^*), \qquad (2.6)$$

where we assume that the surface elevation and the velocity potential are linear superpositions of a steadily propagating unperturbed wave $(\bar{\eta}, \bar{\phi})$ and infinitesimal unsteady perturbations (η', ϕ') where $\eta' \ll \bar{\eta}$ and $\phi' \ll \bar{\phi}$.

Expressions (2.5) and (2.6) are substituted into equations (2.3) and (2.4), which have been transformed into the new frame of reference. The new set is then linearized around the unperturbed wave, and we retain the leading-order (zero-order), which governs the propagating unperturbed wave, and the first-order perturbation equations, which we use to perform the stability analysis.

2.2. *Unperturbed wave solutions*

In the frame of reference (x^*, y^*, z^*, t^*) moving with the wave, the leading-order equations admit steady unperturbed solutions $\bar{\eta}(x,y)$ and $\bar{\phi}(x,y,z)$ of the following form, where asterisks are henceforth omitted for clarity:

$$\left.\begin{array}{l} \bar{\phi}(x,y,z) = -cx + \displaystyle\sum_{i=1}^{\infty} h^i \sum_{m,n} d_{i,mn} \sin{(m\alpha x)}\cos{(n\beta y)}\dfrac{\cosh{[\gamma_{mn}(z+d)]}}{\cosh{(\gamma_{mn}d)}}, \\[14pt] \bar{\eta}(x,y) = \displaystyle\sum_{i=1}^{\infty} h^i \sum_{m,n} c_{i,mn}\cos{(m\alpha x)}\cos{(n\beta y)}, \\[14pt] \omega = \displaystyle\sum_{i=0}^{\infty} h^i\omega_i, \quad \text{where} \quad \gamma_{mn} = (m^2\alpha^2 + n^2\beta^2)^{1/2}. \end{array}\right\} \qquad (2.7)$$
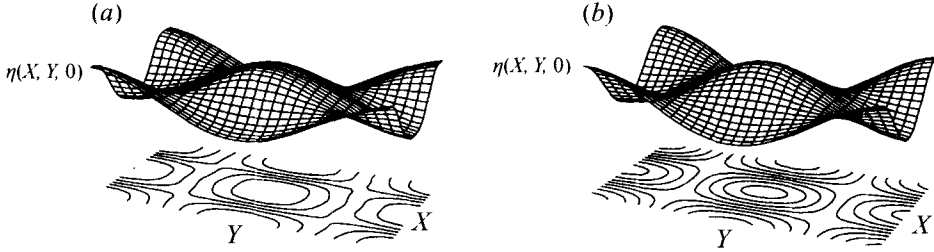
FIGURE 1. Free surfaces and contours of short-crested waves for angle $\theta = 40°$, wave steepness $h = 0.20$, and depths (a) $d = 0.8$ and (b) $d = 2.0$. Surface heights have been magnified.

These solutions represent doubly periodic Fourier series expansions in a small parameter h, the wave steepness, defined as half the non-dimensional peak-to-trough height, since the peak of the wave is fixed at $(x, y) = (0, 0)$:

$$h = \tfrac{1}{2}[\bar{\eta}(0, 0) - \bar{\eta}(\pi, 0)]. \tag{2.8}$$

Truncated expansions have been computed by Marchant & Roberts (1987), using Padé approximation or Shanks transform to attain convergence. The waves admit two two-dimensional limits: $\theta = 90°$ corresponds to finite-depth progressive Stokes waves, whereas $\theta = 0°$ corresponds to finite-depth standing waves. Note that two-dimensional standing waves are derived from these three-dimensional waves, simply by setting $\alpha = 0$ and $\beta = 1$, while two-dimensional progressive waves are not derived from them because non-secularity conditions need to be changed (see Hsu *et al.* 1979). For the standing wave limit, we recovered solutions given by Tadjbakhsh & Keller (1960), while Verma & Keller (1962) did not reach these pure standing wave solutions because they used another dimensionalization, thus changing the non-secularity conditions. In the following study, expansions up to the 35th order have been computed. In figure 1 two surface wave shapes are plotted for a wave steepness $h = 0.20$, angle $\theta = 40°$, and depths $d = 0.8$ and $d = 2.0$. As the water becomes shallower, the high-order terms in the perturbation expansion grow in size (relative to low-order terms), and tend to flatten more of the sea surface while steepening some slopes. This explains the fact that, as the water becomes shallower, the convergence of the perturbation series becomes slower.

The problem of the convergence of our series is a crucial question broadly discussed in Roberts (1983) and Marchant & Roberts (1987). For deep-water flow, Roberts (1983) showed, in a linear description, how a wave harmonic $(\pm J, K)$, i.e. $c_{JK} \sin(J\alpha x) \cos(K\beta y) e^{\gamma_{JK} z}$, travelling at the same phase speed in the x-direction as the fundamental $(\pm 1, 1)$, could grow linearly in time through harmonic resonance. In other words, the harmonic $(\pm J, K)$ is a homogeneous solution of the linear differential equations. These resonances occur under the condition

$$(\alpha^2 J^2 + \beta^2 K^2)^{1/4} = J, \tag{2.9}$$

which is equivalent to the condition of resonance on the angle θ_{HR}:

$$\beta_{HR}^2 = \cos^2 \theta_{HR} = \frac{J^4 - J^2}{K^2 - J^2}. \tag{2.10}$$

Table 1, taken from Roberts (1983), gives 'resonant' angles θ_{HR} for a deep-water flow up to order $N = 15$ of truncation. These critical angles correspond to harmonic

K	$J = 1$	$J = 2$	$J = 3$
3	90.0000	—	—
4	—	0.0000	—
5	90.0000	—	—
6	—	52.2388	—
7	90.0000	—	—
8	—	63.4349	—
9	90.0000	—	00.0000
10	—	69.2952	—
11	90.0000	—	36.6992
12	—	72.9761	—
13	90.0000	—	47.8696
14	—	75.5225	—
15	90.0000	—	54.7356

TABLE 1. Harmonic resonance angles θ_{HR} (in degrees) in deep water up to order of truncation $N = 15$, from Roberts (1983).

resonances of the linear wave ($h = 0$). Considering increasingly higher harmonic resonances, J and $K \rightarrow \infty$, we find that the expansions formally have everywhere a zero radius of convergence. However, for most angles most of these resonances occur at an extremely high order – in a finite truncation the coefficients of the expansions will generally be subject to small divisors (and not to zero divisors). These small divisors cause the expansions to be summable, to some level of accuracy, for wave steepnesses h, so that $h < h^*$, where h^* is the distance to the nearest noticeable resonance. We truncate our series at an order J so that the contributions of all the next orders ($> J+1$) tend to zero (the most important is here of order h^{36}). The remainder $O(h^{J+1})$ does not necessarily tend to zero and thus we cannot assert that our series do converge. However, above h^*, Padé approximation and Shanks transform are used to sum the series: Padé approximants place a simple pole (and a nearby corresponding zero) at the singularities of the expansions in h, which are due to harmonic resonances. They will often converge to a solution of the original expansions for h greater than h^*, see Gilewicz (1978). As mentioned in Roberts (1983), near these pole singularities, due to harmonic resonances, in general three distinct solutions exist, see Roberts (1981). So by crossing h^*, for increasing h, the derived solution will jump from one branch to another. However, Padé approximants select one branch of the solutions and the 'distance' between the different solution branches is of order $h^{max(J, K)/3}$, see Roberts (1983) and Marchant & Roberts (1987) for finite-depth short-crested waves. By truncating the expansions at order 35 and by using Padé approximation one can expect that our solutions $\bar{\eta}(x, y)$ and $\bar{\phi}(x, y, z)$ are approximate short-crested wave fields, although the 'distance' between our solutions and short-crested waves is not estimated in the present study and despite their currently being no rigorous proof of the existence of short-crested waves of permanent form.

2.3. The unsteady perturbations problem

The set of equations of first order, given below, governs the flow of any unsteady perturbations. Note that all partial time derivatives of the unperturbed solutions ($\bar{\eta}, \bar{\phi}$) vanish in this new frame of reference, since it propagates at the same wave speed as the unperturbed wave (in particular, the term $\bar{\phi}_{tz}$, derived from the expansion of ϕ_t around $\bar{\eta}$, vanishes in this propagating frame of reference). This set describes the interaction mechanisms between the steady flow and small unsteady perturbations, in other words

the wave–wave interactions. We compute solutions of this set to determine the instabilities of the basic wave:

$$\nabla^2 \phi' = 0 \quad \text{for} \quad -d \leqslant z \leqslant \bar{\eta}(x, y), \tag{2.11}$$

$$\phi'_z = 0 \quad \text{on} \quad z = -d, \tag{2.12}$$

$$\phi'_t = -\bar{\phi}_x \phi'_x - \bar{\phi}_y \phi'_y - \bar{\phi}_z \phi'_z - (1 + \bar{\phi}_x \bar{\phi}_{xz} + \bar{\phi}_y \bar{\phi}_{yz} + \bar{\phi}_z \bar{\phi}_{zz}) \eta' \tag{2.13}$$

$$\eta'_t = (\bar{\phi}_{zz} - \bar{\eta}_x \bar{\phi}_{xz} - \bar{\eta}_y \bar{\phi}_{yz}) \eta' - \bar{\eta}_x \phi'_x - \bar{\phi}_x \eta'_x - \bar{\eta}_y \phi'_y - \bar{\phi}_y \eta'_y + \phi'_z \tag{2.14}$$

$$\text{on} \; z = \bar{\eta}(x, y).$$

Extending the procedure of IK 93 to finite-depth fluid, we look for non-trivial solutions of (2.11)–(2.14) of the form

$$\binom{\eta'}{\phi'} = e^{-i\sigma t} \left\{ \begin{array}{l} \displaystyle\sum_{J=-\infty}^{\infty} \sum_{K=0}^{\infty} a_{JK}\, e^{i(J\alpha x + K\beta y)} \\[2mm] \displaystyle\sum_{J=-\infty}^{\infty} \sum_{K=0}^{\infty} b_{JK}\, e^{i(J\alpha x + K\beta y)}\, \dfrac{\cosh\left[\kappa_{JK}(z+d)\right]}{\cosh(\kappa_{JK} d)} \end{array} \right\}, \tag{2.15}$$

where $\kappa_{JK} = [(J\alpha)^2 + (K\beta)^2]^{1/2}$.

Since we confine our attention to superharmonic instabilities, the perturbations are chosen to be of the same harmonic structure as the unperturbed flow. Instabilities caused by harmonic resonances correspond to interactions between the two components of the fundamental mode $(\pm 1, 1)$ and two components of a higher harmonic $(\pm J, K)$. The symmetry of the flow with respect to the vertical sea wall allows us to consider $K \geqslant 0$ only.

The stability analysis consists in determining the coefficients a_{JK}, b_{JK} and the set of eigenvalues σ. Since the system of equations (2.11)–(2.14) is real valued, the eigenvalues σ appear in complex-conjugate pairs. Thus an instability corresponds to $\text{Im}(\sigma) \neq 0$. The numerical scheme used for the solution of equations (2.11)–(2.14) is described below.

3. Numerical scheme

The numerical scheme is the extension to finite-depth fluid of the procedure developed by IK 93, 94 for deep water. The series (2.15) are truncated up to harmonics M and N, and the basic wave solutions given by Marchant & Roberts (1987) are obtained up to the 35th order in h, then both expansions are substituted into the surface conditions (2.13) and (2.14). Finally, since unperturbed solutions of permanent form are obtained numerically by an intensive use of Padé approximation, the perturbation equations lead to a homogeneous generalized eigenvalue problem of the form: $Au = i\sigma Bu$, where σ is the set of eigenvalues to be computed with the corresponding eigenvectors $u = (a_{JK}, b_{JK})^t$. A and B are complex matrices, functions of the basic flow. The eigen-analysis is expected to be about as accurate as the numerical solutions for the basic wave – residuals in the equations do not strongly affect the eigen-problem. IK 93, 94 used both collocation and Galerkin methods to solve the eigenvalue problem. They found the latter method to be much more efficient, because it dissociates explicitly the discretization of the collocation points and the order (M, N) of truncation of the eigenmodes. This result has also been noted by Bryant (1985), when computing doubly periodic waves, and later by Zhang & Melville (1987) for the study of the stability of gravity–capillary waves. For that reason, the Galerkin method is used in this paper to solve the eigen-problem. Taking advantage

of the periodicity of both the basic wave solutions and the eigenmodes, equations (2.13) and (2.14) are numerically integrated over one space period in the two horizontal directions using Fourier transforms over a set of $\nu \times \mu$ points whose coordinates are

$$x_u = \frac{2\pi u}{\alpha \nu} \quad \text{for} \quad u = 0, \ldots, \nu - 1, \quad \text{and} \quad y_v = \frac{2\pi v}{\beta \mu} \quad \text{for} \quad v = 0, \ldots, \mu - 1.$$

The following eigen-problem of order $L = 2(2M+1)(2N+1)$ is obtained at $z = \bar{\eta}(x, y)$:

$$\sum_{J=-M}^{M} \sum_{K=0}^{N} F_{J-l, K-r}\{E_{JK}^{(1)}\} a_{JK} + \sum_{J=-M}^{M} \sum_{K=0}^{N} F_{J-l, K-r}\{G_{JK}^{(1)}\} b_{JK} = i\sigma a_{l0}, \qquad (3.1)$$

$$\sum_{J=-M}^{M} \sum_{K=0}^{N} F_{J-l, K-r}\{E_{JK}^{(2)}\} a_{JK} + \sum_{J=-M}^{M} \sum_{K=0}^{N} F_{J-l, K-r}\{G_{JK}^{(2)}\} b_{JK}$$

$$= i\sigma \sum_{J=-M}^{M} \sum_{K=0}^{N} F_{J-l, K-r}\{H_{JK}\} b_{JK}, \qquad (3.2)$$

where

$$E_{JK}^{(1)} = \{-\bar{\phi}_{zz} + iJ\alpha\bar{\phi}_x + iK\beta\bar{\phi}_y + \bar{\eta}_x \bar{\phi}_{xz} + \bar{\eta}_y \bar{\phi}_{yz}\},$$

$$G_{JK}^{(1)} = \{(\bar{\eta}_x J\alpha i + \bar{\eta}_y K\beta i)\cosh[\kappa_{JK}(\bar{\eta} + d)] - \kappa_{JK}\sinh[\kappa_{JK}(\bar{\eta} + d)]\}\frac{1}{\cosh(\kappa_{JK} d)},$$

$$E_{JK}^{(2)} = \{1 + \bar{\phi}_x \bar{\phi}_{xz} + \bar{\phi}_y \bar{\phi}_{yz} + \bar{\phi}_z \bar{\phi}_{zz}\},$$

$$G_{JK}^{(2)} = \{(\bar{\phi}_x J\alpha i + \bar{\phi}_y K\beta i)\cosh[\kappa_{JK}(\bar{\eta} + d)] + \kappa_{JK}\bar{\phi}_z\sinh[\kappa_{JK}(\bar{\eta} + d)]\}\frac{1}{\cosh(\kappa_{JK} d)},$$

$$H_{JK} = \frac{\cosh[\kappa_{JK}(\bar{\eta} + d)]}{\cosh(\kappa_{JK} d)}.$$

The functions

$$F_{J-l, K-r}\{f_{JK}\} = \sum_{u=0}^{\nu-1} \sum_{v=0}^{\mu-1} f_{JK}\, e^{i\alpha(J-l)x_u}\, e^{i\beta(K-r)y_v},$$

where $l = -M, \ldots, M$ and $r = -N, \ldots, N$, are computed using two-dimensional fast Fourier transforms. The integers ν and μ are increased until the Fourier coefficients converge; thus the surface perturbation is consistently described. Convergence of the eigenvalues and eigenvectors is then obtained by increasing M and N. The reader should refer to IK 93 to get full numerical and computational details of the method, since the numerical scheme is little changed in extending it to finite-depth water. It is also worth noting that an increase of the order of truncation past the 35th order does not affect the convergence of the eigenvalue problem until depth $d = 0.5$. The runs are sequential and each one creates the parameters for the next run. A standard sequence requires about twenty runs. Thus, the use of a CRAY-YMP supercomputer, with special attention given to the vectorization of the numerical code, was necessary since a standard run takes five minutes.

4. Numerical analysis

4.1. *Introduction*

IK 93, in performing a stability analysis, discovered that harmonic resonances correspond to class Ia(J, K) superharmonic 'bubbles' of instability, which are very weak and sporadic in the wave steepness range (see IK 94 for a definition of three-

dimensional classes of instability associated with symmetric short-crested waves). They explained these resonances as a process involving a collision of two superharmonic modes (J, K) and $(-J, K)$ at zero frequency (phase locked with the unperturbed wave: $\mathrm{Re}(\sigma) = 0$ for both superharmonic eigenmodes). The authors found that for deep water, the growth rates ($|\mathrm{Im}(\sigma)|$) are lower than h^{2J}, and occur over a range of h (for which $\mathrm{Re}(\sigma) = 0$) of width smaller than h^{2J} for the strongest instabilities. Since the lowest-order harmonic resonances correspond to $J = 2$ (see table 1), i.e. resonances $(\pm 2, 4)$, $(\pm 2, 6)$, $(\pm 2, 8)$, ..., (i) the strongest instabilities have growth rates of order lower than h^4, so that they are weak compared to subharmonic instabilities (of order h^2), and (ii) the h-range of instability (the h-width of the 'bubble') is at most of order h^4 as well, so that these superharmonic instabilities are sporadic. They found restabilization past the bubble of instability, as the frequencies leave the zero-frequency axis. Each instability bubble is centred on an h-value which is very close to the pole of the truncated series calculated by Roberts (1983). One should refer to IK 93 for a description of the collision mechanisms, as they are the same for finite-depth water.

These resonances still exist for finite-depth water. They are generated when harmonic $(\pm J, K)$, i.e. $c_{JK} \sin(J\alpha x)\cos(K\beta y)\cosh[\gamma_{JK}(z+d)]/\cosh(\gamma_{JK}d)$, is a solution of the homogeneous linear differential equations governing the finite-depth flow. The new condition of harmonic resonance is then

$$\gamma_{JK}\tanh(\gamma_{JK}d) = J^2\tanh(d).\tag{4.1}$$

Table 2 gives angles of resonance θ_{HR}, in the linear case, for three depths $d = 2$, 1 and 0.5 up to the harmonic $N = 15$. For all depths, tables 1 and 2 have in common: (i) an infinite number of resonances at $\theta = 90°$ ($J = 1$), and (ii) as the order N of truncation increases, the number of harmonic resonances increases. For $N \to \infty$, a resonance, and hence zero divisor, will occur arbitrarily near every angle between $\theta = 0°$ and $90°$, in a linear description. Therefore the perturbation series has an everywhere zero radius of convergence. However IK 93 showed that, for nonlinear short-crested waves, high-order harmonic resonances need not be considered, since the growth rates in their instability bubble are not significant.

The purpose of the present study is to analyse numerically the stability of finite-depth short-crested water waves to superharmonic perturbations, in order to provide accurate time scales (proportional to the inverse growth rates) of these harmonic resonances and to analyse the contribution of the depth parameter d. The new harmonic resonances, appearing because of the finite depth d, are also analysed, in particular those associated with the standing wave limit, $\theta = 0°$. These particular resonances are given in table 3 up to the order $N = 20$ of truncation and are calculated from the resonance condition

$$J^2 = K\frac{\tanh(Kd)}{\tanh(d)}.\tag{4.2}$$

4.2. Stability analysis

For $h = 0$, the unperturbed wave is given by $\bar{\eta} = 0$ and $\bar{\phi} = -c_0 x$ with $c_0 = \omega_0/\alpha = \tanh^{1/2}(d)/\alpha$. Then the eigenvalues are

$$\sigma_{JK}^s = -(J\alpha)c_0 + s[\kappa_{JK}\tanh(\kappa_{JK}d)]^{1/2}, \quad s = \pm 1,\tag{4.3}$$

where the signature of the perturbation is defined as $\mathrm{sign}[s\,\mathrm{Im}(-\mathrm{i}\sigma)]$, see MacKay & Saffman (1986). The set of eigenvalues $\{\sigma_{JK}^s\}$ is neutrally stable for $h = 0$. Instabilities may arise when the wave steepness h is non-zero. We use the approach of IK 93, which

	K	J = 1	J = 2	J = 3	J = 4
(a)	3	90.0000	—	—	—
	4	—	71.8333	—	—
	5	90.0000	—	40.3734	—
	6	—	78.9931	—	—
	7	90.0000	—	61.1950	—
	8	—	81.9849	—	25.9592
	9	90.0000	—	68.9529	—
	10	—	83.6713	—	46.1829
	11	90.0000	—	73.2648	—
	12	—	84.7627	—	56.5926
	13	90.0000	—	76.0594	—
	14	—	85.5295	—	62.3353
	15	90.0000	—	78.0331	—
(b)	3	90.0000	—	—	—
	4	—	48.0500	—	—
	5	90.0000	—	—	—
	6	—	65.8354	—	—
	7	90.0000	—	12.9790	—
	8	—	72.6052	—	—
	9	90.0000	—	43.4217	—
	10	—	76.3291	—	—
	11	90.0000	—	54.3842	—
	12	—	78.7137	—	—
	13	90.0000	—	60.8416	—
	14	—	80.3795	—	30.9155
	15	90.0000	—	65.2072	—
(c)	3	90.0000	—	—	
	4	—	17.8737	—	
	5	90.0000	—	—	
	6	—	54.3511	—	
	7	90.0000	—	—	
	8	—	64.8095	—	
	9	90.0000	—	16.3751	
	10	—	70.3369	—	
	11	90.0000	—	39.7124	
	12	—	73.8210	—	
	13	90.0000	—	49.9385	
	14	—	76.2354	—	
	15	90.0000	—	56.3629	

TABLE 2. Harmonic resonance angles θ_{HR} (in degrees) for finite depth flow up to order $N = 15$ of truncation for depths (a) $d = 0.5$, (b) $d = 1.0$, (c) $d = 2.0$.

takes advantage of the work of MacKay & Saffman (1986) on Hamiltonian systems, and we apply the necessary condition for instability in terms of eigenvalue collisions of opposite signatures (s) or at zero frequency. An instability can arise if, for some wave steepness h, two modes have the same frequency:

$$\sigma^s_{J1\,K1}(h) = \sigma^{-s}_{J2\,K2}(h). \tag{4.4}$$

After substituting (4.3) into (4.4), and bearing in mind that a harmonic resonance (J, K) corresponds to a collision of two eigenmodes (J, K) and $(-J, K)$, i.e. $K_1 = K_2 = K$ and $J_1 = -J_2 = J$, we obtain

$$\kappa_{JK} \tanh(\kappa_{JK} d) = J^2 \alpha^2 c_0^2 = J^2 \tanh(d), \tag{4.5}$$

which is equivalent to condition (4.1). In the case of standing wave harmonic resonances, at angle $\theta = 0°$, for which $\alpha = 0$, $\beta = 1$, and so $\kappa_{JK} = K$, we simply obtain (4.2).

These instabilities belong to class Ia $(m = J, K)$ and, in a fixed frame of reference, they can be interpreted as a resonance between the two eigenmodes k_1 and k_2 and the $2m$-components k_{01} and k_{02} of the unperturbed wave:

$$\Omega_1 = -\Omega_2 + J\Omega_{01} + J\Omega_{02}, \tag{4.6}$$

$$k_1 = k_2 + Jk_{01} + Jk_{02}, \tag{4.7}$$

with $\Omega_i = |k_i|^{1/2}\tanh^{1/2}(d\kappa_{JK})$, and $\Omega_{0i} = |k_{0i}|^{1/2}\tanh^{1/2}(d\kappa_{11})$, for $i = 1, 2$, and $k_1 = (J\alpha, K\beta)^t$, $k_2 = (-J\alpha, K\beta)^t$, $k_{01} = (\alpha, \beta)^t$, $k_{02} = (\alpha, -\beta)^t$. Once the poles of the expansion series have been calculated using Padé approximation, we perform the computations in their vicinity: the maximum growth rates and bands of instability in h are then determined by solving the eigenvalue problem.

5. Numerical results

IK 93 showed that the strongest superharmonic instabilities for deep water are of class Ia $(J = 2, K)$. We focus our numerical study on the harmonic resonance $(\pm 2, 6)$, bearing in mind that, apart from $(\pm 2, 4)$, all other $(\pm 2, K)$ resonances are of higher order, and the $(\pm J, K)$ resonances for $J > 2$, are weaker, see IK 93. For that reason, it is not necessary to carry out an extensive parametric study over a wide range of harmonic resonances $(\pm J, K)$, depths d and wave steepnesses h. We present a partial answer to the following crucial question: is a short-crested wave field, perturbed by superharmonic perturbations, observable? In other words, is a perturbed field such as this, likely to keep its harmonic shape unchanged (without taking modulational variations into consideration)? The study of superharmonic instabilities provides us with their time scales, and thus we determine whether the high-order harmonics of the perturbed wave can become dominant compared to its fundamental mode, or whether the fundamental wave keeps its harmonic structure nearly unchanged.

Two-dimensional Stokes waves are primarily unstable to subharmonic modulational instabilities. These waves are not subject to superharmonic instabilities, except near breaking and except for the weak and sporadic instabilities identified by Kharif & Ramamonjiarisoa (1988, 1990), so that, without taking modulational instabilities into account, they are observable. IK 93 named the perturbed short-crested waves on deep water *quasi-permanent* because the associated superharmonic instabilities are very weak and 'sporadic' compared to the dominant modulational instabilities. For that reason, they are not likely to develop, except over very long time scales: the variation of this wave field due to harmonic resonances is very slow in time. For the case of finite-depth short-crested waves, the study of $(\pm 2, 6)$ resonance will provide us with such information, since it is one of the strongest harmonic resonances, see IK 93.

5.1. *Harmonic resonance in experiments*

In figure 2 are plotted linear (for $h = 0$) harmonic resonance curves derived from equation (4.1) in the (d, θ)-plane for the most significant harmonic resonances (low-order resonances): only resonances $(\pm 3, 9)$, $(\pm 2, 4)$, $(\pm 2, 6)$, $(\pm 2, 8)$ and $(\pm 2, 10)$ are considered in this section; resonances $(\pm 4, 6)$, $(\pm 3, 5)$ and $(\pm 3, 7)$ corresponding to the standing wave limit are analysed in §5.3. Experiments of Hammack *et al.* (1989) are also reported for reference. In this section we concentrate on the parameter regime in
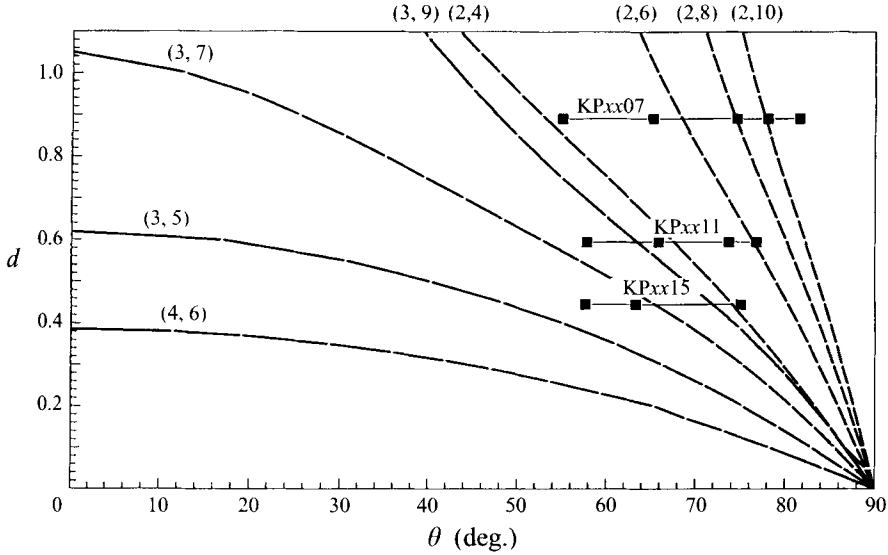
FIGURE 2. Location of linear harmonic resonances for the strongest instabilities $(\pm 2, 4)$, $(\pm 2, 6)$, $(\pm 2, 8)$, $(\pm 2, 10)$, $(\pm 3, 5)$, $(\pm 3, 7)$, $(\pm 3, 9)$ and $(\pm 4, 6)$. Experiments of Hammack *et al.* (1989) are also shown for comparison: KPxx07, KPxx11 and KPxx15 with xx increasing from right to left.

the right-hand half of the figure; a region encompassing the experiments and where the harmonic resonances are generally of low order. In this parameter regime, the region of instability associated with the $(\pm J, K)$ resonance occurs immediately to the right of the curve labelled (J, K), see IK 93; for a given depth d, a harmonic resonance on finite-amplitude waves can appear only for angles greater than the associated angle of resonance θ_{HR} – the bubble of instability occurring in some range of h-values. Angle θ increases from θ_{HR} with the h-position of the centre of the bubble: since a harmonic resonance is physically meaningful only for h smaller than the value h_{max} for which the wave is breaking, the resonance can be observed only near the range of θ such that $\theta_{HR} < \theta < \theta_b = \theta_{HR} + \delta\theta$, where θ_b represents the angle at which the bubble of instability should appear at the wave steepness corresponding to the maximum wave steepness of the wave considered. Thus, $\delta\theta$ would be the width of the band of instability to the right of the curves in figure 2 for a given depth d. $\delta\theta$ is approximately $2°$ in deep water, $1.2°$ for $d = 1$ and $0.2°$ for $d = 0.5$. These approximate values are not reported in figure 2 because they are extrapolated from our computations (up to $h = 0.30$ wave steepness) using the highest-wave steepnesses of short-crested waves given by Marchant & Roberts (1987). While increasing θ from θ_{HR} to $\theta_{HR} + \delta\theta$, the centre of the bubble of instability shifts from zero to h_{max}. The extremely weak θ-band of instability might be the reason why Hammack *et al.* (1989) have not directly observed these instabilities. Moreover an experiment may lie in the narrow band and yet may not be the location of a superharmonic instability if the experimental wave steepness does not fit the numerical one (the width of the bubbles is given in §5.3). This point may be demonstrated by the following example: for harmonic resonance $(\pm 2, 6)$ and depth $d = 1$, the angle of resonance is $\theta_{HR} = 65.8354°$ at wave steepness $h = 0$; for angle $\theta = 66.2°$ the maximum growth rate (0.32×10^{-2}) is obtained at wave steepness $h = 0.194$, and for angle $\theta = 66.3°$ it is of amplitude 0.13×10^{-1} and is obtained at wave steepness $h = 0.299$. Obviously an uncertainty of $0.1°$ for θ in experiments can lead to an uncertainty of $\delta h = 0.10$ for the wave steepness required to observe an harmonic
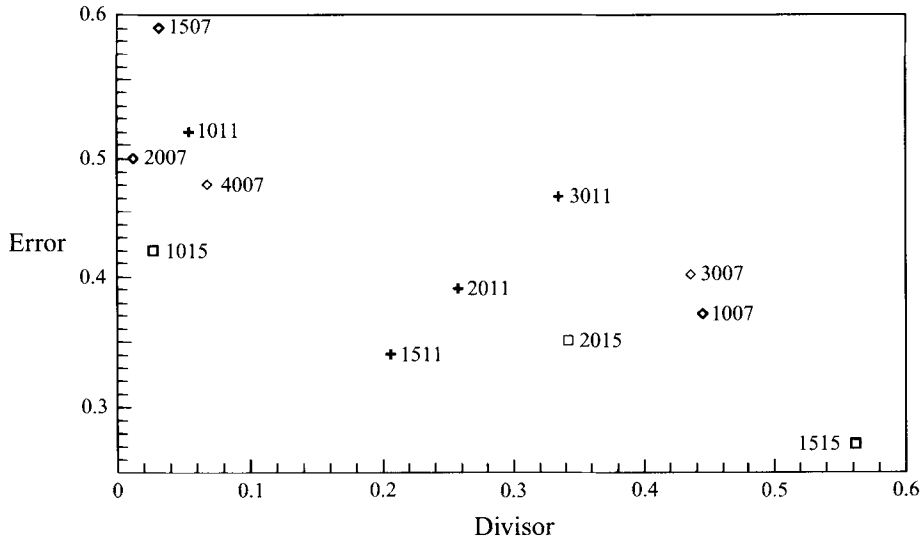
FIGURE 3. For each of the experiments of Hammack *et al.* (1989), a plot of the r.m.s. error versus distance from harmonic resonance as measured by the divisor from equation (4.1). Each experiment is associated with resonance as follows: KP1007 (± 2, 10); KP1507 (± 2, 10); KP2007 (± 2, 8); KP3007 (± 2, 4); KP4007 (± 2, 4); KP1011 (± 2, 6); KP1511 (± 2, 4); KP2011 (± 3, 9); KP3011 (± 3, 7); KP1015 (± 2, 4); KP1515 (± 3, 5); and KP2015 (± 3, 5).

resonance. This clearly shows that the experimental wave steepness may lie outside the theoretical bubble of instability that is predicted by the present computations owing to experimental uncertainties.

However, a detailed examination of the data reported by Hammack *et al.* (1989) implicates harmonic resonance in some of the features of their results. Consider the error of their fit of data to genus 2 solutions of the Kadomtsev–Petviashvili (KP) equation. In the regime of the experiments, the effects of harmonic resonance lie primarily to the right of the curves drawn in figure 2. Thus, as listed in the caption to figure 3, we identified which low-order resonance plotted in figure 2 lies immediately to the left of the different experimental parameter values. Then we crudely estimate the importance of that resonance by computing the divisor that would appear in an asymptotic expansion, namely the difference between the right-hand and left-hand sides of (4.1). For each experiment listed in table 2 by Hammack *et al.* (1989), we plot in figure 3 their r.m.s. error versus the computed divisor. Observe the clear decrease in error with distance from resonance as measured by the divisor. This trend is also strong in the KPxx07 and KPxx15 series of experiments when each series is considered separately – one reason for the lower level in overall error for the KPxx15 series is that the wave steepness of these experiments, approximately $kf_{max}/2 \approx 0.08$, is lower than the wave steepness, approximately 0.18, of the KPxx07 experiments.

There is also evidence of the resonance in the time traces shown in figure 9(*c*) of Hammack *et al.* (1989). Computing the period of the harmonic we estimate that there should be approximately 2.1 cycles of the excited harmonic per cycle of the fundamental wave. It is not hard to imagine that many of the deviations from theory that are recorded in the experiment have twice the frequency of the fundamental (especially at gauges 2 to 6). The other traces shown in their figure 9 are not suitable for showing resonance: trace (a) is of experiment KP1515 which has been identified as the furthest from resonance; and (b) is of KP1007 for which an involvement with (2,
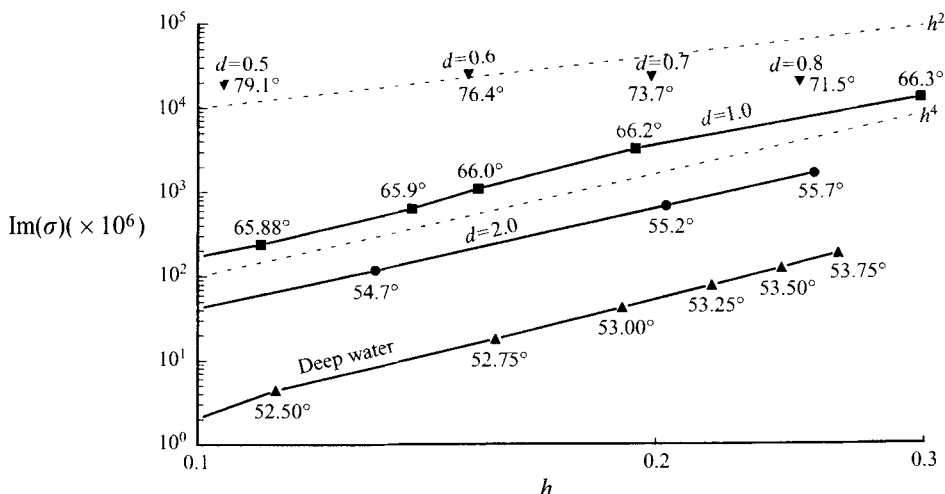
FIGURE 4. The maximum growth rates versus the wave steepness h for superharmonic instabilities of class Ia ($J = 2$, $K = 6$) in a log–log plot. Results for seven depths are reported (there is only one isolated point for depths $d = 0.8$, 0.7, 0.6, 0.5).

10) resonance is the most dubious owing to its relatively high order. In summary, the experiments show faint but strongly suggestive evidence of the influence of harmonic resonance.

5.2. *The* (2, 6) *resonance*

Figure 4 shows growth rates of the (2, 6) resonance for different depths ($d \to \infty$, $d = 2$, 1, 0.8, 0.7, 0.6 and 0.5) and an example of the bubble of instability is displayed in figure 5 ($\theta = 65.9°$ for which $\theta_{HR} = 65.8354°$). The dashed curves h^2 and h^4 are added for reference, since they are the maximum growth rates of modulational instabilities and superharmonic instabilities for deep-water short-crested waves, respectively, see IK 93, 94. As the water becomes shallower, the superharmonic instabilities become considerably stronger. This result is not surprising, since high-order harmonics (associated with harmonic resonances) become larger in amplitude with decreasing depth. Moreover, for depths around $d = 0.5$, superharmonic instabilities have growth rates of order h^2 comparable to those of classes Ia, b ($J = 1, K = \pm 1$) modulational instabilities in deep water computed by IK 94. This result is important, since it suggests that short-crested waves, perturbed by superharmonic modes in finite depth, can no longer be quasi-permanent although the bands of instability are of very limited extent in the parameter d, θ, h space.

From this study, we think that the best way to localize these instabilities experimentally is to increase very slightly angle θ, starting from θ_{HR}, for a given depth and wave steepness in order to ensure that the h-band of instability has been covered. Considering the limited size of the experimental tunnel, small depths (around $d = 0.5$), i.e. high growth rates, are obviously more suitable.

One feature to note in the experiments of Hammack *et al.* (1989), is that any forced harmonic wave generally escapes out of their short-crested wave field through the sides. Some simple ray theory indicates that the temporal growth rates in an infinite field (reported herein), when translated to spatial growth rates in a finite field, width w, are not only reduced by the sideways 'leakage' but only become apparent as a spatial instability if the temporal growth rate is above the threshold $\pi c_y / (2w)$, where c_y is the transverse component of the group velocity of the harmonic wave. For the experiments
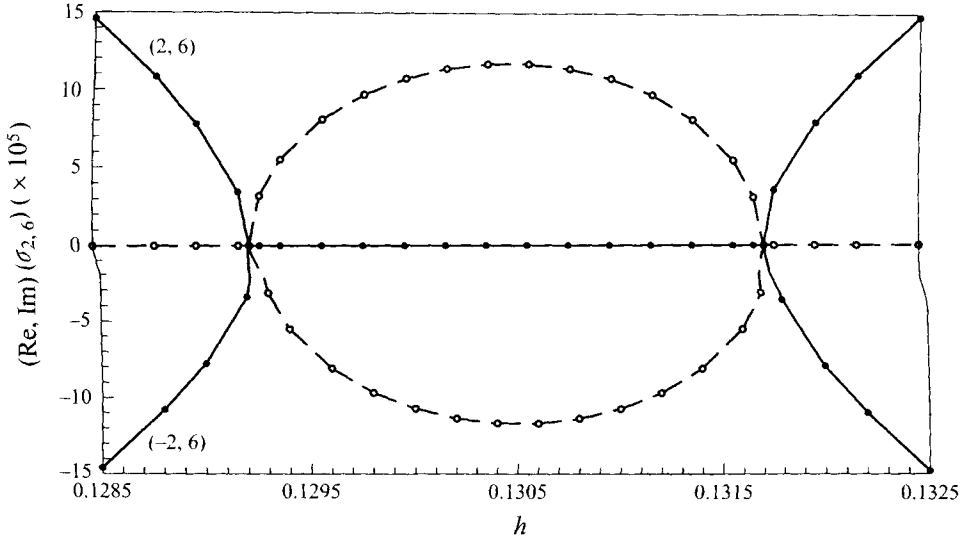
FIGURE 5. Frequency (solid line) and growth rate (dashed line) for (± 2, 6) perturbations as a function of wave steepness h for angle $\theta = 65.9°$.

of Hammack *et al.* (1989) this threshold is roughly 0.01 s^{-1} and so for the wave steepnesses used in the experiments, in the range 0.08–0.2, our figure 4 indicates that only the strongest instabilities could have been observed. Instabilities should be more easily observed in a wave tank where the short-crested wave field spans the entire width and where reflecting walls trap any generated harmonic.

5.3. *Instabilities associated with standing waves*

Table 3, taken from Marchant & Roberts (1987), gives depth values for harmonic resonances in the standing wave limit, $\theta = 0°$. Some aspects of their effects on standing waves are shown in figures 2–5 in Mercer & Roberts (1994). In this section, we study the strongest (lowest-order) superharmonic instabilities ($\pm 3, 5$), in the vicinity of the depth $d_{HR} = 0.624$, where d_{HR} represent in the linear case depths associated with harmonic resonances given in table 3 for $\theta = 0°$; *in figure 2 are plotted resonances* (± 3, 5), (± 3, 7) *and* (± 4, 6) *associated with the standing wave limit in the linear case versus angle θ*. In figure 6 are plotted the frequencies of perturbations (± 3, 5), for two depths $d = 0.61$ and 0.59 close to d_{HR}, for a flat surface ($h = 0$). For $\theta \geq \theta_0$ or depth d deeper than d_{HR}, no superharmonic instability is observed on increasing the wave steepness from zero. In these cases, frequencies 'repulse' each other, avoiding any collision at zero frequency (see figure 7). For $0° < \theta < \theta_0$, and for water shallower than d_{HR}, a bubble of instability arises. As the depth decreases, the critical angle θ_0 shifts to increasing values of θ, until it reaches $\theta = 90°$ for $d \to 0$. As a result, the instabilities associated with the standing wave limit spread over the entire θ-range ($0°$–$90°$) as the depth d decreases. Unlike the instabilities described in the previous subsection, on the left-hand side of the figure finite-amplitude resonances are located immediately to the left of, or below, the resonant curves (as also shown for the (5, 13) standing wave resonance in figure 3 of Mercer & Roberts 1994). For a given angle $\theta(\theta < \theta_0)$, a decrease of depth d from $d = d_{HR}$ will increase the wave steepness for which the bubble of instability arises. Instabilities associated with standing wave harmonic resonances, those listed in table 3, then appear only for depths such that $d_b = d_{HR} - \delta d < d < d_{HR}$, where d_b represents the depth for which the bubble of instability arises at a wave
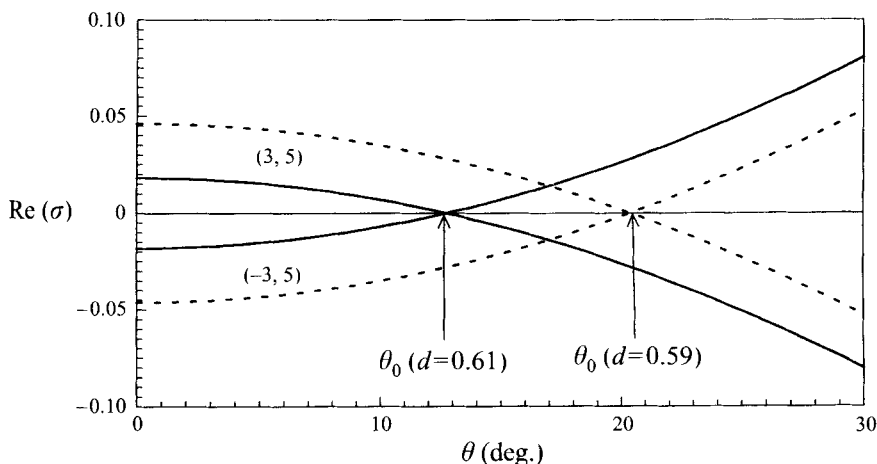
FIGURE 6. Frequencies of the perturbation harmonics (± 3, 5) at zero wave steepness as a function of angle θ, referred to harmonic resonance depth $d_{HR} = 0.624$: $d = 0.61$ (solid line), $d = 0.59$ (dashed line).

K	J = 2	J = 3	J = 4	J = 5	J = 6	J = 7	J = 8	J = 9	J = 10	J = 11	J = 12	J = 13
4	∞	—	—	—	—	—	—	—	—	—	—	—
5	—	0.624	—	—	—	—	—	—	—	—	—	—
6	—	—	0.386	—	—	—	—	—	—	—	—	—
7	—	1.040	—	0.275	—	—	—	—	—	—	—	—
8	—	—	0.550	—	0.211	—	—	—	—	—	—	—
9	—	∞	—	0.357	—	0.169	—	—	—	—	—	—
10	—	—	0.734	—	0.284	—	0.139	—	—	—	—	—
11	—	—	—	0.473	—	0.226	—	0.118	—	—	—	—
12	—	—	0.973	—	0.347	—	0.186	—	0.101	—	—	—
13	—	—	—	0.577	—	0.272	—	0.157	—	—	—	—
14	—	—	1.354	—	0.441	—	0.222	—	0.135	—	—	—
15	—	—	—	0.694	—	0.317	—	0.186	—	0.118	—	—
16	—	—	∞	—	0.478	—	0.256	—	0.160	—	0.104	—
17	—	—	—	0.830	—	0.362	—	0.213	—	0.139	—	—
18	—	—	—	—	0.550	—	0.290	—	0.182	—	0.123	—
19	—	—	—	0.997	—	0.410	—	0.239	—	0.158	—	0.110
20	—	—	—	—	0.627	—	0.324	—	0.203	—	0.139	—

TABLE 3. Depths d_{HR} (> 0.1) at which harmonic resonance occurs for standing waves $\theta = 0°$ up to order $N = 20$ of truncation, from Marchant & Roberts (1987).

steepness corresponding to the breaking wave steepness of the wave considered. For harmonic resonance (± 3, 7), and by extrapolating our results further to $h = 0.2$, δd is roughly of order 0.1 near $\theta = 0°$.

Figure 8 shows growth rates as function of angle θ for two depths $d = 0.61$ and 0.59. The growth rates attain their maximum value for $\theta \to 0°$. From this result, one can say that the primary instability of finite-depth water waves close to the standing wave limit is superharmonic, whereas, see Mercer & Roberts (1992), deep-water standing waves are dominated by subharmonic instabilities. The other important result is that these instabilities appear to spread and 'contaminate' the whole 0°–90° range of θ as the depth decreases although progressive waves, the extreme of θ (90°), are unaffected, in accordance with results of McLean (1982b). However, this contamination is not
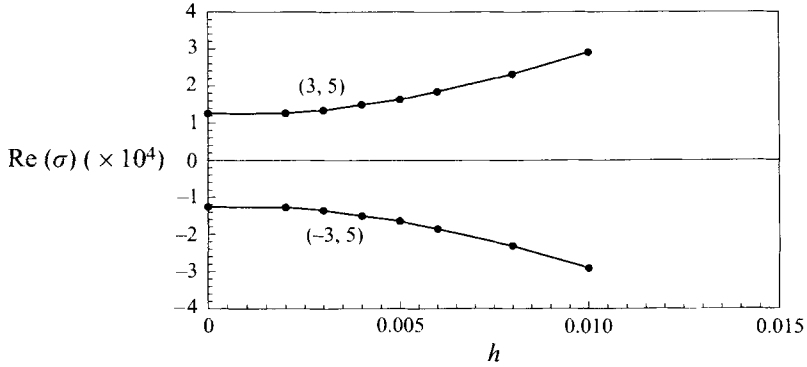
FIGURE 7. Frequencies of the perturbation harmonics (± 3, 5) as a function of the wave steepness h for depth $d = 0.61$ with angle $\theta = 12.80°$ ($\theta > \theta_0$ ($d = 0.61$) $= 12.75°$, see figure 4).
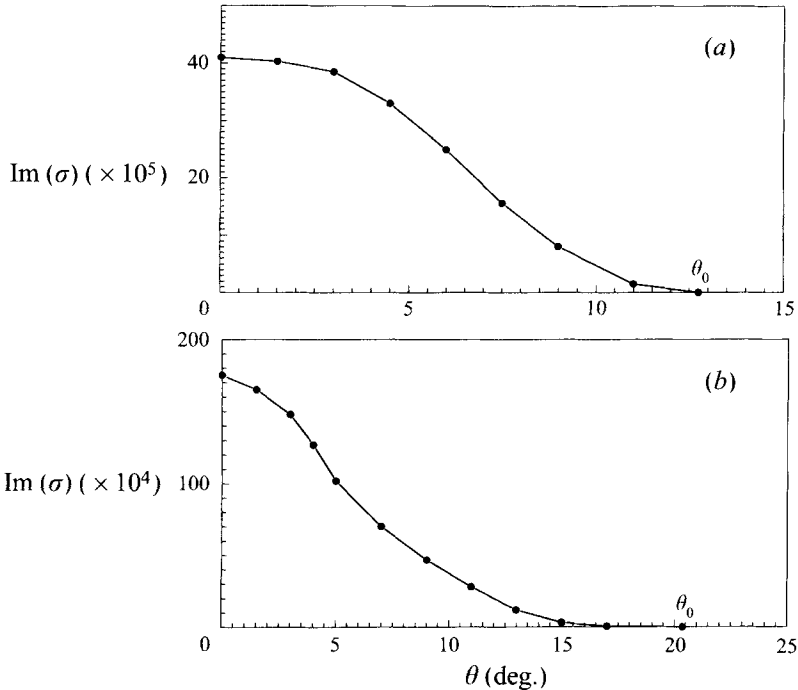

FIGURE 8. The maximum growth rates versus angle θ, for superharmonic instabilities of class Ia ($J = 3, K = 5$). These plots refer to harmonic resonance depth $d_{HR} = 0.624$: (a) $d = 0.61$, (b) $d = 0.59$.

necessarily relevant over the whole θ-span for $0° < \theta < \theta_0$, since the maximum growth rates are significantly only in the vicinity of $\theta = 0°$. In particular, these particular instabilities are not likely to be evident in the experiments of Hammack et al. (1989) as the experiments are located in regions of the (d, θ)-plane where these superharmonic instabilities are either not present or very weak (see figure 8).

Figure 9 shows growth rates of the same instability versus the wave steepness h. We have used in this figure the data from figure 8. They are of the same order as those measured in the previous subsection. Each point represents the maximum of the growth rate of the instability for a given angle between $\theta \to 0$ and $\theta = \theta_0$ (see figure 6). The largest h-values are determined by $\theta \to 0$. As θ is increased, the maximum growth
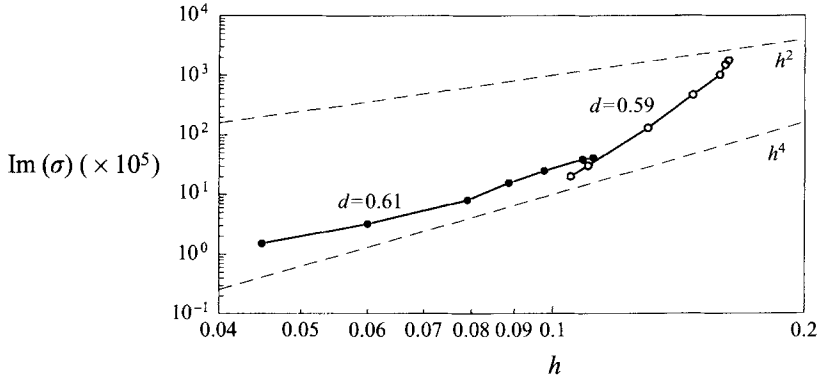
FIGURE 9. The maximum growth rates versus the wave steepness h for class Ia ($J = 3$, $K = 5$) superharmonic instabilities in a log–log plot; results for two depths close to the harmonic resonance depth $d_{HR} = 0.624$.

rate decreases with the corresponding h-location of the bubble of instability. For that reason, it is not practically possible to directly compare growth rates for two different depths at the same wave steepness h. However, one can see that the considerable increase of the inclination of the two curves in figure 9 for two similar depths (0.61 and 0.59) suggests that depth is a major aspect; one can expect a greater growth rate for shallower water. For that reason, for both kinds of superharmonic instabilities, the growth rates and h-ranges of instability can be higher than h^2 (generally the h-widths of the bubbles are of the same order as the maximum growth rates), even for depths reasonably close to d_{HR}, and can become more significant with depth d decreasing. This suggests that for shallower depths and for high wave steepness, the h-range of instability will cover almost the whole h-span up to breaking for every $(\pm J, K)$ resonance, so that we can no longer talk about sporadic bubbles of instability in terms of the wave steepness h as in the deep-water case. However, since the band of instability in the (d, θ)-plane is limited, these bubbles remain sporadic with respect to d and θ. From table 3, one can conclude that for water shallower than approximately $d = 1$ and in certain range of δd, waves close to three-dimensional standing waves cannot have permanent form since a strong superharmonic instability arises for $d < 1.040$, through the $(\pm 3, 7)$ harmonic resonance in the standing wave limit.

6. Conclusions

The work presented here deals with the stability of three-dimensional short-crested waves to superharmonic instabilities on water of finite depth. As in the case of deep water, these class Ia instabilities are associated with the harmonic resonance phenomena described by Roberts (1983) and Marchant & Roberts (1987). In shallow water, these instabilities are no longer negligible, since they may be stronger than deep-water subharmonic instabilities (of order h^2). However, the most significant instabilities cover a very localized region of the (d, θ)-plane, so that we can reasonably consider that short-crested waves and long-crested waves 'close' to progressive two-dimensional waves are observable in general.

Superharmonic instabilities associated with the standing wave limit are also quantified. We found that these instabilities spread out over the entire fully three-dimensional flow regime, except for two-dimensional Stokes waves, with maximum growth rates occurring for waves 'close' to standing waves. From our computations,

it is suggested that long-crested waves 'close' to two-dimensional standing waves, perturbed by superharmonic instabilities, are not observable for some depths shallower than approximately a non-dimensional depth $d = 1$.

It will be of interest to compare these results to those of subharmonic instabilities by comparing the respective time scales: as water becomes shallower, waves become less and less dispersive, which suggests that subharmonic modulational instabilities will become weaker than those in deep water. Because of the patterns of growth rates which we have determined, one can say that localized superharmonic instabilities will become more important in shallower water. Further study on the subharmonic instabilities will determine which instability (superharmonic or subharmonic) is dominant.

REFERENCES

BADULIN, S. I., SHRIRA, V. I., KHARIF, C. & IOUALALEN, M. 1995 On two approaches to the problem of instability of short-crested water waves. *J. Fluid Mech.* **303**, 297–325.

BRYANT, P. J. 1985 Doubly periodic progressive permanent waves in deep water. *J. Fluid Mech.* **161**, 27–42.

CHAPPELEAR, J. E. 1961 On the description of short-crested waves. *Beach Erosion Board, US Army Corps Engrs Tech. Memo*, 125.

FUCHS, R. A. 1952 On the theory of short-crested oscillatory gravity waves. *US Natl Bur. Stand. Circular* **521**, 187–200.

GILEWICZ, J. 1978 *Approximants de Padé*. Lecture Notes in Mathematics, vol. 667. Springer.

HAMMACK, J., McCALLISTER D., SHEFFNER, N. & SEGUR, H. 1995 Two-dimensional periodic waves in shallow water. Part 2. Asymmetric waves. *J. Fluid Mech.* **285**, 95–122.

HAMMACK, J., SCHEFFNER, N. & SEGUR, H. 1989 Two-dimensional periodic waves in shallow water. *J. Fluid Mech.* **209**, 567–589.

HAMMACK, J., SCHEFFNER, N. & SEGUR, H. 1991 A note on the generation and narrowness of periodic rip current. *J. Geophys. Res.* **96**, 4909–4914.

HSU, J. R. C., TSUCHIYA, Y. & SILVESTER, R. 1979 Third-order approximation to short-crested waves. *J. Fluid Mech.* **90**, 179–196.

IOUALALEN, M. 1993 Fourth order approximation of short-crested waves. *CR Acad. Sci.* Paris **316** (II), 1193–1200.

IOUALALEN, M. & KHARIF, C. 1993 Stability of three-dimensional progressive gravity waves on deep water to superharmonic disturbances. *Eur. J. Mech.* B **12**, 401–414 (referred to herein as IK 93).

IOUALALEN, M. & KHARIF, C. 1994 On the subharmonic instabilities of steady three-dimensional deep water waves. *J. Fluid Mech.* **262**, 265–291 (referred to herein as IK 94).

KHARIF, C. & RAMAMONJIARISOA, A. 1988 Deep water gravity wave instabilities at large steepness. *Phys. Fluids* **31**, 1286–1288.

KHARIF, C. & RAMAMONJIARISOA, A. 1990 On the stability of gravity waves on deep water. *J. Fluid Mech.* **218**, 163–170.

MACKAY, R. S. & SAFFMAN, P. G. 1986 Stability of water waves. *Proc. R. Soc. Lond.* A **406**, 115–125.

MARCHANT, T. R. & ROBERTS, A. J. 1987 Properties of short-crested waves in water of finite depth. *J. Austral. Math. Soc.* B **29**, 103–125.

McLEAN, J. W. 1982*a* Instabilities of finite amplitude water waves. *J. Fluid Mech.* **114**, 315–330.

McLean, J. W. 1982*b* Instabilities of finite amplitude gravity waves on water of finite depth. *J. Fluid Mech.* **114**, 331–341.

Mercer, G. N. & Roberts, A. J. 1992 Standing waves in deep water: their stability and extreme form. *Phys. Fluids* A **4**, 259–269.

Mercer, G. N. & Roberts, A. J. 1994 The form of standing waves on finite depth water. *Wave Motion* **19**, 233–244.

Peregrine, D. H. 1985 Water waves and their development in space and time. *Proc. R. Soc. Lond.* A **400**, 1–17.

Phillips, O. M. 1960 On the dynamics of unsteady gravity waves of finite amplitude. *J. Fluid Mech.* **9**, 193–217.

Roberts, A. J. 1981 The behaviour of harmonic resonant steady solutions to a model differential equation. *Q. J. Mech. Appl. Maths* **34**, 287–310.

Roberts, A. J. 1983 Highly nonlinear short-crested water waves. *J. Fluid Mech.* **135**, 301–321.

Roberts, A. J. & Peregrine, D. H. 1983 Notes on long-crested waves. *J. Fluid Mech.* **135**, 323–335.

Roberts, A. J. & Schwartz, L. W. 1983 The calculation of nonlinear short-crested gravity waves. *Phys. Fluids* **26**, 2388–2392.

Tadjbakhsh, I. & Keller, J. B. 1960 Standing surface waves of finite amplitude. *J. Fluid Mech.* **8**, 442–451.

Verma, G. R. & Keller, J. B. 1962 Three-dimensional standing surface waves of finite amplitude. *Phys. Fluids* **5**, 52–56.

Zhang, J. & Melville, W. K. 1987 Three-dimensional instabilities of nonlinear gravity–capillary waves. *J. Fluid Mech.* **174**, 187–208.